ELSEVIER

Journal of Chromatography B, 769 (2002) 323–332

JOURNAL OF CHROMATOGRAPHY B

www.elsevier.com/locate/chromb

Proteomic analysis of rat soleus and tibialis anterior muscle following immobilization

Robert J. Isfort[a,*], Feng Wang[a], Kenneth D. Greis[a], Yiping Sun[b], Thomas W. Keough[b], Sue C. Bodine[c], N. Leigh Anderson[d]

[a]*Research Division, Health Care Research Center, Procter & Gamble Pharmaceuticals, 8700 Mason-Montgomery Rd., Mason, OH 45040-9317, USA*

[b]*Corporate Research Division, Procter & Gamble, Ross, OH, USA*

[c]*Regeneron Pharmaceuticals, Tarrytown, NY, USA*

[d]*Large Scale Biology Corporation, Germantown, MD, USA*

Received 8 August 2001; received in revised form 7 January 2002; accepted 7 January 2002

Abstract

A proteomic analysis was performed comparing normal slow twitch type fiber rat soleus muscle and normal fast twitch type fiber tibialis anterior muscle to immobilized soleus and tibialis anterior muscles at 0.5, 1, 2, 4, 6, 8 and 10 days post immobilization. Muscle mass measurements demonstrate mass changes throughout the period of immobilization. Proteomic analysis of normal and atrophied soleus muscle demonstrated statistically significant changes in the relative levels of 17 proteins. Proteomic analysis of normal and atrophied tibialis anterior muscle demonstrated statistically significant changes in the relative levels of 45 proteins. Protein identification using mass spectrometry was attempted for all differentially regulated proteins from both soleus and tibialis anterior muscles. Four differentially regulated soleus proteins and six differentially regulated tibialis anterior proteins were identified. The identified proteins can be grouped according to function as metabolic proteins, chaperone proteins, and contractile apparatus proteins. Together these data demonstrate that coordinated temporally regulated changes in the proteome occur during immobilization-induced atrophy in both slow twitch and fast twitch fiber type skeletal muscle.

Keywords: Proteomic analysis; Muscles; Proteins

1. Introduction

Skeletal muscle atrophy is a process by which skeletal muscle, in response to a variety of stimuli, selectively loses proteins [1–5]. Skeletal muscle atrophy can be induced by diverse stimuli such as disuse, immobilization, denervation, sepsis, and starvation [1–5]. While each atrophy-inducing mechanism has its own unique initiation signal, it is generally believed that a common mechanism for the reduction of contractile protein loss occurs. The selective loss of a subset of skeletal muscle proteins including contractile proteins results in muscles with smaller myofibers but no loss of myofiber numbers [1–5]. It is generally thought that atrophy and hypertrophy are physiological mechanisms that func-

*Corresponding author. Tel.: +1-513-622-1899; fax: +1-513-622-1195.

E-mail address: isfortrj@pg.com (R.J. Isfort).

1570-0232/02/$ – see front matter
PII: S1570-0232(02)00021-1

tion to meet the work demand placed on the muscle and to store and release amino acids during times of physiological need.

Skeletal muscle atrophy occurs both by decreasing protein synthesis and increasing protein degradation [6–9]. Mechanistically, this occurs by altering both gene transcription and mRNA translation and by modulating several proteolytic systems including the calpain, lysosomal and ubiquitin-mediated proteolytic systems [6–9]. While contractile proteins are somewhat selectively lost during skeletal muscle atrophy, additional non-contractile proteins are also lost [1]. Thus the process of skeletal muscle atrophy is probably more complex than what has been previously recognized. Multiple types of muscle, based on the type of contractile and metabolic protein isoforms expressed in the muscle and the nature of the physiological response of the muscle, have been described. These include slow twitch fiber type muscle as exemplified by the soleus muscle, fast twitch fiber type muscle as exemplified by the tibialis anterior muscle and mixed slow and fast type fiber muscle as exemplified by the medial gastrocnemius muscle; each general classification of fiber type can be further subdivided depending on the metabolic nature of the fiber, i.e. oxidative metabolism, glycolytic metabolism, etc. [10]. Skeletal muscle atrophy of all fiber types occurs during atrophy if disuse of the muscle occurs and it is generally believed that the process of atrophy is independent of fiber type [10].

Proteomics refer to a collection of technologies with the common goal of separating and identifying proteins in complex biological samples. One of the most widely used proteomic technologies is two-dimensional gel electrophoresis (2DGE). 2DGE involves separating a complex protein mixture first by charge using isoelectric focusing then by size using SDS–PAGE. Coupling these two technologies allows for the separation of approximately 100–1000 s of proteins into discrete spots, a level of separation that is very useful for many biological applications [11]. Importantly, 2DGE can be performed so that quantitation of the relative levels of the separated proteins is possible, even between unrelated samples, thus allowing 2DGE to be used to understand changes in protein expression in response to a perturbation of a biological system [11]. When 2DGE is coupled with a protein identification technology, such as Edman sequencing or mass spectrometry, proteins of interest can be identified and an understanding of the biological significance of the protein changes can be determined. Thus proteomic analysis has the potential to provide not only data, but also knowledge, with regards to a biological process.

In order to gain a better understanding of the protein changes that occur during immobilization-induced atrophy in both slow twitch and fast twitch fiber types, a proteomic analysis was performed on soleus and tibialis anterior muscle undergoing immobilization atrophy. The results of that analysis are reported here.

2. Experimental

2.1. Immobilization-induced atrophy

Rat right hindlimb immobilization was performed using the pin-heel method as has been described previously [12]. At the indicated times, three animals per time point were euthanized by CO_2 asphyxiation followed by cervical dislocation, the right soleus and tibialis anterior muscles were dissected from the hindlimb, cleaned of tendons and connective tissue, weighed and snap frozen in cyogenic vials by immersion in liquid nitrogen. Muscles were stored at −80 °C until processed.

2.2. Sample preparation

Soleus and tibialis anterior muscles were prepared for two-dimensional gel electrophoresis (2DGE) as follows. Frozen soleus and tibialis anterior muscles were crushed to a fine powder in liquid nitrogen using a mortar and pestle, 0.1 g of tissue was solubilized in 0.4 ml of solubilization buffer (9 *M* urea, 2% CHAPS, 0.5% dithiothreitol, 2% pH 8.0–10.5 Pharmalytes), the solubolized tissue was homogenized and shaken for approximately 30 min then centrifuged for 30 min; finally the supernatant was removed and aliquoted for analysis.

2.3. Two-dimensional electrophoresis

Sample proteins were resolved by 2DGE using the 20×25 cm ISO-DALT 2-D gel system (Large Scale Biology Corporation, Germantown, MD) essentially as described previously [13–15]. All first dimension isoelectric focusing gels were prepared using the same single standardized batch of ampholytes (BDH 4-8A) by combining urea, ampholytes and acrylamide solution to cast the tube gels; casting the tube gels and allowing to polymerize for at least 1 h; loading the tube gel into the isoelectric focusing apparatus and adding buffer; and prefocusing the gel for 1 h at 200 V. Eight microliters of solubilized muscle protein were applied to each tube gel and the gels were run for 25 050 V h using a progressively increasing voltage protocol implemented by a programmable high voltage power supply as described previously [13–15]. Eight microliters of solubilized muscle protein was empirically determined to be an appropriate amount of protein for optimal protein resolution and visualization without overloading. An Angelique computer controlled gradient casting system was used to prepare second dimension SDS gradient slab gels in which the top 5% of the gel was 11% T acrylamide and the lower 95% of the gel varies linearly from 11 to 18% T. The first-dimensional IEF tube gels were loaded directly onto the slab gels without equilibration and held in place by agarose. Second dimension slab gels were run in groups of 20 in thermal-regulated DALT tanks with buffer circulation. Following SDS electrophoresis, slab gels were stained for protein using a colloidal Coomassie Blue G-250 procedure involving fixation in 50% ethanol/2% phosphoric acid overnight, three 30-min washes in cold deionized water, transfer to 34% methanol/17% ammonium sulfate/2% phosphoric acid for 1 h followed by addition of 1 g/1.5 l of powdered Coomassie Blue G-250 stain and staining for 4 days. Samples were analyzed at least twice—if adequate resolution was not achieved on one of the gels, additional gel runs were performed.

2.4. Quantitative computer analysis

Each stained slab gel was digitized in red light at 133 μm resolution using an Eikonix 1412 scanner. Each 2-D gel was processed using the Kepler software system to yield a spotlist giving position, shape and density information for each detected spot. This procedure makes use of digital filtering, mathematical morphology techniques and digital masking to remove background and uses full two-dimensional least squares optimization to refine the parameters of a 2-D Gaussian shape for each spot. Each 2-D pattern was matched to an appropriate soleus and tibialis anterior muscle ''master'' 2-D pattern. The master map was created by running a number of soleus and tibialis anterior muscle samples multiple times in order to derive an averaged image. This image was then used as a standard for matching all subsequent gel images. In the matching, a series of about 50 proteins was matched by an experienced operator working with a montage of all the 2-D patterns in the experiment. Subsequently, an automatic program matched additional spots to the master pattern using as a basis the manual landmark data entered by the operator. After the automatic matching, the operator inspected matching for errors. The groups of gels making up an experiment were scaled together by a linear procedure based on a selected set of spots. These spots were selected by a procedure that chooses spots that have been matched in at least 80% of the gels. All gels in the experiment were then scaled together by setting the summed abundance of the selected spots equal to a constant. A Student's *t*-test was used to evaluate the level of significance of any quantitative change in the level of analyzed proteins between control and each time point after the induction of atrophy. A response was considered significant if the difference between control and any time point achieved the $P<0.01$ significance level ($n=3$ per protein spot per time point).

2.5. Protein identification

Protein spots of interest were excised from the Coomassie Blue-stained gels and in-gel tryptic digestion performed [16,17]. Briefly, the spots were washed with 100 m*M* NH_4HCO_3/50% CH_3CN several times followed by reduction and alkylation with DTT and iodoacetamide, respectively. After washing with 100 m*M* NH_4HCO_3/50% CH_3CN,

0.15–0.2 μg of porcine trypsin in 100 m*M* NH_4HCO_3 was added to the gel pieces followed by an overnight incubation at 30 °C. Protein identification was performed using MALDI–MS as follows. Mass spectrometry of the tryptic fragments was performed by mixing the peptides from in-gel trypsin digestion with an equal volume of saturated α-cyano-4-hydroxycinnamic acid matrix dissolved in 50% CH_3CN/0.3% TFA, then spotted onto a MALDI–TOF target plate. Peptide spectra were collected on a PerSeptive Biosystems, Voyager DE-STR MALDI–TOF mass spectrometer in the positive ion, reflector mode with delayed ion extraction using the following conditions: nitrogen laser at 337 nm, accelerating voltage at 20 kV, grid voltage at 73%, ion delay at 100 ns and a mass range of 800–3800 Da. The mono-isotopic masses were calibrated to internal, auto-digestion peptides from porcine trypsin at 842.5100 and 2211.1046 such that the unknown peptide masses were accurate to within 25 ppm. Protein identification was facilitated using the MS-FIT module of the ProteinProspector (ver. 3.2.1) program, supplied by PerSeptive Biosystems. The accurate tryptic, monoisotopic peptide masses were searched against the entire NCBI database to match with tryptic peptide masses from known proteins and/or predicted protein from DNA sequences. All spectra were internally calibrated using two spiked peptides and databases searched with a mass tolerance of 25 ppm.

In the event that the protein identification was ambiguous after the MALDI–TOF step, the remaining peptide sample was analyzed by capillary LC–ESI-MS–MS with an LCPackings Ultimate capillary LC system equipped with a FAMOS micro-autosampler and a 5 cm×300 μm I.D. PepMap C_{18} column coupled to a Finnigan LCQ^{Deca} ion-trap mass spectrometer. A gradient was developed over 30 min at 4 μl/min from 2 to 49% acetonitrile containing 0.1% formic acid to elute the peptides from the column directly into the mass spectrometer. Data were collected and analyzed using Finnigan Xcalibur ver. 1.2 software in data-dependent scan mode such that any peptide signal over 1×10^5 intensity triggered the automated acquisition of an MS–MS fragmentation spectrum for that peptide. The collective MS–MS spectra for each capillary LC–MS–MS run were searched against the NCBI database using Mascot Daemon (ver. 1.7.1) as a client attached to an in-house Mascot search protocol server (http://www.matrixscience.com).

3. Results

3.1. Soleus and tibialis anterior muscle mass changes during immobilization

Atrophy of the soleus and tibialis anterior muscles was induced by right hindlimb immobilization using the pin-heel method. Soleus and tibialis anterior muscles were removed from the right leg of three control rats as well as the right leg of immobilized rats (three per time point) at 0.5, 1, 2, 4, 6, 8 and 10 days post immobilization. All removed soleus and tibialis anterior muscles were weighed and prepared for 2D gel analysis. The changes in soleus muscle mass following immobilization are presented in Fig. 1A. Two major periods of mass loss occurred, one between 0 and 0.5 days post immobilization and one between 4 and 6 days post immobilization, with approximately 50% of muscle mass lost by 10 days of immobilization. The changes in tibialis anterior muscle mass following immobilization are presented in Fig. 1B. Similar to what was seen with the soleus muscle, two major periods of muscle loss occurred—one occurring between 0 and 0.5 days post immobilization and one occurring between 6 and 8 days post immobilization, with approximately 50% of muscle mass lost by 10 days of immobilization.

3.2. Changes in soleus and tibialis anterior muscle protein levels following hindlimb immobilization

Proteomic analysis of normal and immobilized soleus and tibialis anterior muscle proteins was performed at 0, 0.5, 1, 2, 4, 6, 8, and 10 days post immobilization. The normal soleus and tibialis anterior muscle protein pattern was used to create a soleus and tibialis anterior muscle proteome master map that was subsequently used for landmarking and identifying proteins whose relative levels change following immobilization. As can be seen in Fig. 2A, 17 soleus muscle proteins with statistically significant changes in relative abundance (at the $P<0.01$ level) were identified (these proteins are denoted by

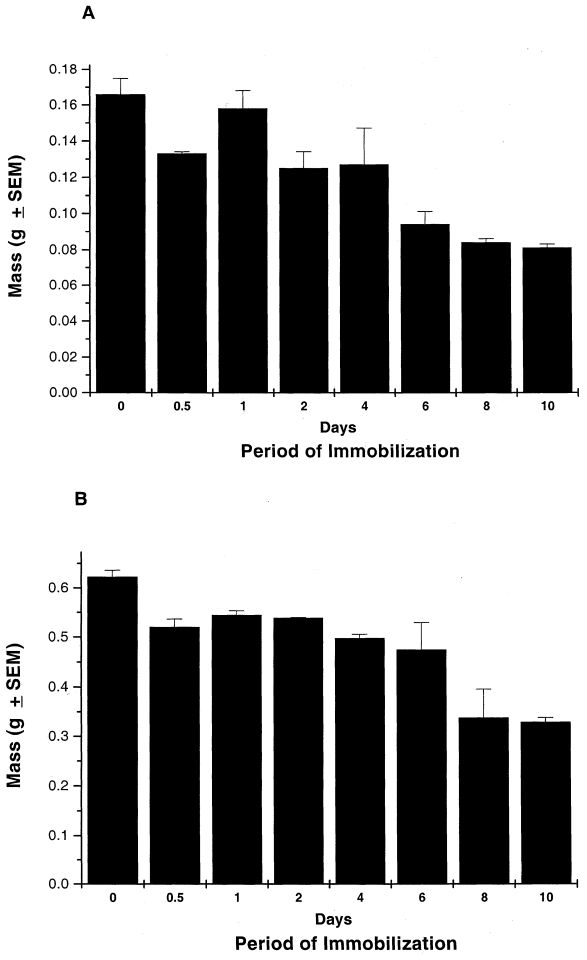

Fig. 1. Analysis of rat soleus and tibialis anterior muscle mass changes following hindlimb immobilization. For immobilization, the right hindleg of a rat was immobilized using the pin-heel technique and soleus and tibialis anterior muscles were removed at 0, 0.5, 1, 2, 4, 6, 8, and 10 days post immobilization and weighed ($n=3$ for each time point). (A) Immobilized soleus mass data; (B) immobilized tibialis anterior mass data.

their coordinate numbers and dark shading relative to all proteins resolved—represented by light shading). These proteins cover a broad range of molecular masses, isoelectric points and abundance levels (the size of the spot indicates relative abundance). Fig. 2B demonstrates the relative level of change in the 17 soleus muscle proteins at varying times following immobilization. Each tick separates a group of three protein spots (the same protein) with each protein spot coming from a different soleus muscle with the three different soleus muscles coming from three different animals. Several different patterns of change are observed including a gradual increase in relative protein abundance (a total of six spots—spots 38, 140, 262, 280, 322, 656); a gradual decrease in relative protein abundance (a total of two spots—spots 333 and 450); a sharp increase in relative protein abundance between 6 and 8 days post immobilization (spot 201); a sharp decrease in relative protein abundance between 0 and 0.5 days post immobilization (a total of five spots—spots 444, 515, 621, 829, 1997); and other changes in relative protein abundance (the remaining three spots).

Changes in the relative levels of tibialis anterior proteins are demonstrated in Fig. 3A. As can be seen in Fig. 3A, 45 tibialis anterior muscle proteins with statistically significant changes in relative abundance (at the $P<0.01$ level) were identified (these proteins are denoted by their coordinate numbers and dark shading relative to all proteins resolved—represented by light shading). These proteins cover a broad range of molecular masses, isoelectric points and abundance levels (the size of the spot indicates relative abundance). Fig. 2B demonstrates the relative level of change in the 45 tibialis anterior muscle proteins at varying times following immobilization. Each tick separates a group of three protein spots (the same protein) with each protein spot coming from a different tibialis anterior muscle with the three different tibialis anterior muscles coming from three different animals. Several different patterns of change are observed including a gradual increase in relative protein abundance (a total of six spots—spots 314, 322, 376, 1048, 1260, 1949); a sharp increase in relative protein abundance between 0 and 0.5 days post immobilization (a total of 19 spots—spots 29, 59, 88, 154, 186, 268, 269, 294, 321, 339, 343, 379, 386, 426, 452, 461, 521, 691, 1918); a sharp decrease in relative protein abundance between 0 and 0.5 days post immobilization followed by a sharp increase between 0.5 and 1 day post immobilization (a total of five spots—spots 107, 120, 129, 140, 192); a sharp increase in relative protein abundance between 8 and 10 days post immobilization (a total of two spots—spots 1177 and 1502); a sharp increase in relative protein abundance between 0 and 0.5 days post immobilization and between 8 and 10 days post immobilization (a total of four

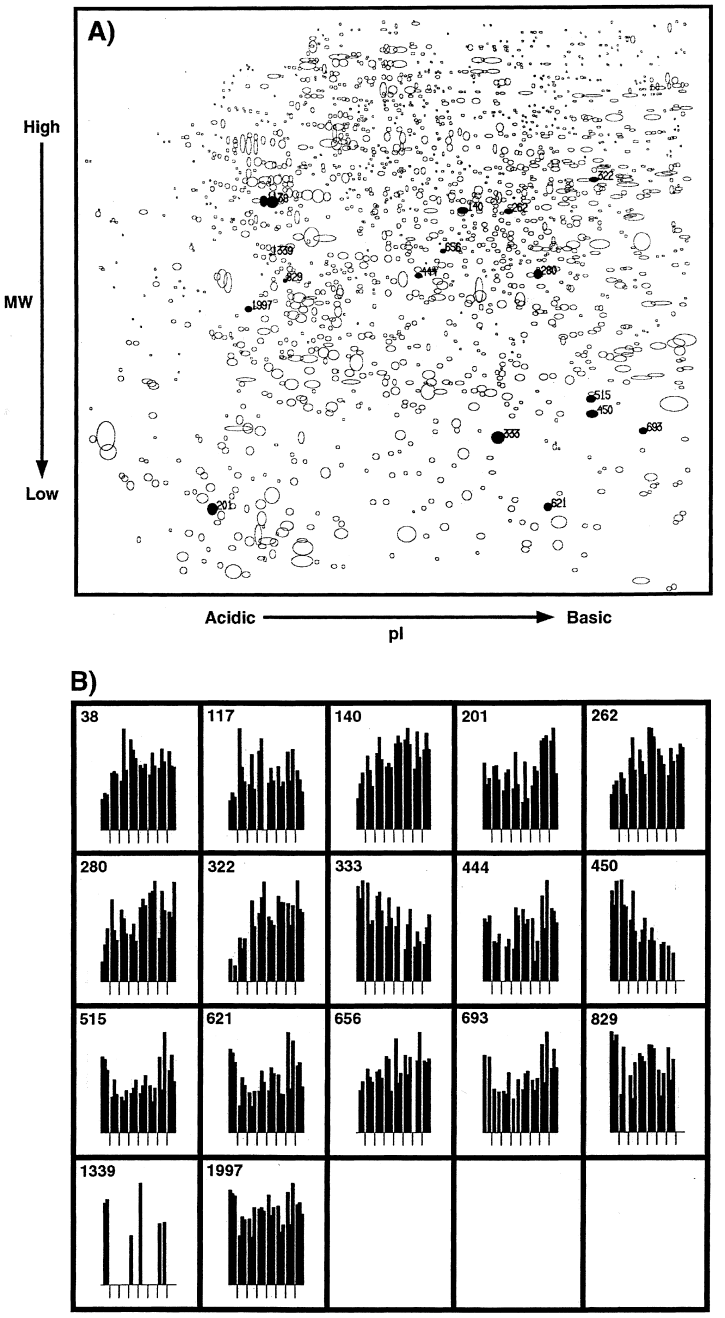

Fig. 2. Alterations in the relative levels of soleus muscle proteins following right hindlimb immobilization. Soleus muscle proteins were prepared and fractionated by 2D gel electrophoresis as described in the Experimental section. (A) Master map of soleus muscle proteins (clear spots) showing proteins with statistically significant changes in relative levels of expression following immobilization (black spots). (B) Graphical representation of the 17 soleus proteins with statistically significant changes in relative level of expression following hindleg immobilization. Each tick separates a group of three protein spots (the same protein), each from a different soleus muscle from three different animals. Time points following immobilization are identified by each tick mark (from left to right—0, 0.5, 1, 2, 4, 6, 8, and 10 days post immobilization). Each panel, which represents the integrated Coomassie Blue absorbance measurement for one protein, is the relative measure of the normalized abundance of that protein from the different experimental groups (*y*-axis) versus experimental group (*x*-axis).

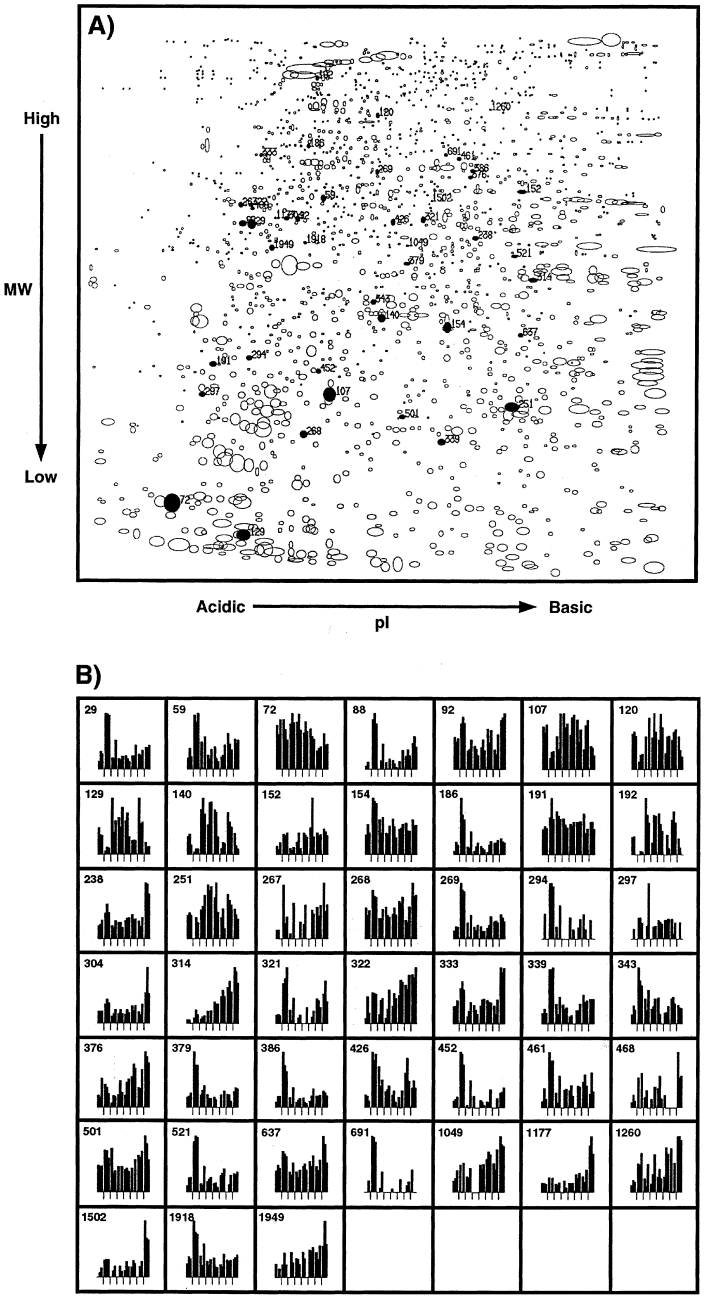

Fig. 3. Alterations in the relative levels of tibialis anterior muscle proteins following right hindleg immobilization. Tibialis anterior muscle proteins were prepared and separated by 2D gel electrophoresis as described in the Experimental section. (A) Master map of tibialis anterior muscle proteins (clear spots) showing proteins with statistically significant changes in relative levels of expression following immobilization (black spots). (B) Graphical representation of the 45 tibialis anterior proteins with statistically significant changes in relative level of expression following hindleg immobilization. Each tick separates a group of three protein spots (the same protein), each from a different tibialis anterior muscle from three different animals. Time points following immobilization are identified by each tick mark (from left to right—0, 0.5, 1, 2, 4, 6, 8, and 10 days post immobilization). Each panel, which represents the integrated Coomassie Blue absorbance measurement for one protein, is the relative measure of the normalized abundance of that protein from the different experimental groups (y-axis) versus experimental group (x-axis).

spots—spots 92, 238, 268, 333); and other changes in relative protein abundance (the remaining nine spots). Importantly, the visual clustering of proteins by similar temporal changes indicates that coordinated regulation of the levels of selective groups of proteins occurred.

3.3. Protein identification

Protein identification using MALDI–TOF and LC–MS–MS was attempted for all proteins demonstrating statistically significant changes in relative protein levels during immobilization-induced atrophy. Table 1 provides the protein identification for four soleus and six tibialis anterior proteins with altered levels of relative abundance during immobilization-induced atrophy. The four soleus proteins include H^+ transporting ATP synthase beta chain (protein S280), P20 (protein S333), alpha B crystalline (protein S450) and carbonic anhydrase III (protein S515); the six tibialis anterior proteins include H^+ transporting ATP synthase beta chain (protein TA29), heat shock protein 60 precursor (protein TA59), myosin alkali light chain 1 (protein TA72), desmin (protein TA92), phosphoglucomutase (protein TA152) and antioxidant protein 2 (protein TA501). All other proteins from the atrophied soleus and tibialis anterior muscles were either unable to be identified (provided no useful mass spectra) or were novel proteins—proteins which produced useful mass spectra without a match in the protein database. Importantly, our attempts to identify proteins were hampered by an unknown contaminant in the gels that interfered with the mass identification and greatly reduced our sensitivity of detection.

The altered proteins can be grouped into three classes based on their functions. For example, one class is metabolic proteins—proteins that function, in general, in some area of cellular metabolism. This includes H^+ transporting ATP synthase beta chain (soleus protein S280 and tibialis anterior protein TA29), carbonic anhydrase III (soleus protein S515), phosphoglucomutase (tibialis anterior protein TA152), and antioxidant protein 2 (tibialis anterior protein TA501). In our previous studies on denervation and hindlimb suspension-induced atrophy, we observed changes in H^+ transporting ATP synthase beta chain and carbonic anhydrase III [18,19]. Of these two proteins, H^+ transporting ATP synthase beta chain seems to be the most commonly altered protein since it is observed to change in both the soleus and tibialis anterior muscles in denervation, immobilization and hindlimb suspension-induced atrophy. Thus control of the relative levels of this protein may be important during the atrophy process. In addition, because the H^+ transporting ATP synthase beta protein is altered in all models of atrophy, it may be a useful marker of skeletal muscle atrophy. Carbonic anhydrase may also be a useful marker of skeletal muscle atrophy since the relative levels of this protein were observed to be altered in both denervation and immobilization-induced atrophy in the soleus muscle [18,19]. A second class of proteins includes contractile apparatus or cytoskeletal proteins. Included in this class are the myosin alkali light chain 1 protein (tibialis anterior protein TA72) and desmin (tibialis anterior protein TA92). In our previous studies of denervation and hindlimb suspension-induced atrophy, alterations in contractile proteins have been observed; alteration of this class of proteins is expected since contractile apparatus proteins are the target of much of the proteolysis observed during atrophy [10]. Finally, a third class of proteins that are collectively known as chaperone or heat shock proteins were altered during immobilization-induced atrophy. Included in this class of proteins were P20 (soleus protein S333), alpha B crystallin (soleus protein S450), and heat shock protein 60 (tibialis anterior protein 60). Chaperone proteins were found to be altered during denervation and hindlimb suspension-induced atrophy [18,19]. Alteration of this class of proteins may be expected since chaperone proteins are believed to participate in the quasi-crystalline ordering of the contractile apparatus and thus are probably lost to proteolytic cleavage at the same time as the contractile apparatus. Because of the consistency of alteration of chaperone/heat shock proteins in different models of atrophy, these proteins may serve as useful markers of atrophy. Interestingly, Naito et al. [20] recently demonstrated that maintenance of chaperone/heat shock proteins at their preatrophy levels during disuse atrophy attenuates the loss of muscle mass and protein observed during atrophy. Thus the loss of chaperone/heat shock proteins during atrophy may be a critical step in the atrophy process and

Table 1
Protein identification of soleus and tibialis anterior proteins demonstrating relative expression level changes during immobilization

Protein Spot Number	Protein Identification	MOWSE or SEQUEST* Xcorr/dCN score	Peptides Matched	Predicted MW/p*I*	Soleus or Tibialis Anterior
S280	H^+ transporting ATP synthase beta chain	1440	TIAMDGTEGLVR IMNVIGEPIDER AHGGYSVFAGVGER FTQAGSEVSALLGR VALTGLTVAEYFR VALVYGQMNEPPGAR LVLEVAQHLGESTVR	51.2 kDa/4.9	Soleus
S333	P20	867	VPVQPSWLR VVGDHVEVHAR ASAPLPGFSTPGR RASAPLPGFSTPGR HEERPDEHGFIAR	17.5 kDa/6.1	Soleus
S450	Alpha B crystallin	3.07/0.3*	HFSPEELK	20.1 kDa/6.8	Soleus
S515	Carbonic anhydrase III	1330	GGPLSGPYR YNTFGEALK VVFDDTFDR YAAELHLVHWNPK EPMTVSSDQMAKLR VVFDDTFDRSMLR EKGEFQILLDALDK HDPSLQPWSVSYDPGSAK	29.4 kDa/6.4	Soleus
TA29	H^+ transporting ATP synthase beta chain	3200	IMNVIGEPIDER AHGGYSVFAGVGER FTQAGSEVSALLGR VALTGLTVAEYFR VALVYGQMNEPPGAR LVLEVAQHLGESTVR IMDPNIVGSEHYDVAR VLDSGAPIKIPVGPETLGR DQEGQDVLLFIDNIFR AIAELGIYPAVDPLDSTSR	51.2 kDa/4.9	Tibialis anterior
TA59	Heat shock protein 60 precursor	1.98/0.26* 1.8/0.22* 1.52/0.05*	VGLQVVAVK LSDGVAVLK IGIEIIK	60.9 kDa/5.9	Tibialis anterior
TA72	Myosin alkali light chain 1	3.61/0.42* 3.51/0.39* 3.11/0.35* 2.86/0.3* 2.64/0.35* 2.58/0.41* 2.47/0.41* 2.0/0.38*	DQGGYEDFVEGLR ITLSQVGDVLR HVLATLGEK EAFLLFDR VFDKEGNGTVMGAELR ALGTNPTNAEVK SFSADQIAEFK EGNGTVMGAELR	16.5 kDa/4.6	Tibialis anterior
TA92	Desmin	3.1/0.45* 3.01/0.46* 1.92/0.07*	TSGGAGGLGSLR ADVDAATLAR FANYIEK	53.5 kDa/5.2	Tibialis anterior
TA152	Phosphoglucomutase	2.94/0.45* 2.92/0.38* 1.75/0.15* 1.49/0.11*	IDAMHGVVGPYVK DLEALMLDR LYIDSYEK NIFDFNALK	61.4 kDa/6.3	Tibialis anterior
TA501	Antioxidant protein 2	2.13/0.19*	NFDEILR	24.8 kDa/5.6	Tibialis anterior

modulation of the loss of heat shock proteins may be a novel mechanism to prevent skeletal muscle atrophy.

4. Conclusions

Proteomic analysis of soleus (slow twitch) and tibialis anterior (fast twitch) muscle undergoing immobilization-induced atrophy has demonstrated that multiple proteins undergo changes in their relative level of expression. These changes are coordinated and affect proteins involved in metabolic, contractile and chaperone functions. These results demonstrate the utility of proteomic analysis in: (1) understanding a complex biological process such as skeletal muscle atrophy; (2) providing potential targets for therapeutic intervention; and (3) provide insight into the post-genomic mechanisms of protein expression modification that occur during the process of skeletal muscle atrophy.

References

[1] G.J. Herbison, M.M. Jaweed, J.F. Ditunno, Arch. Phys. Med. Rehabil. 60 (1979) 401.
[2] D.F. Goldspink, Biochem. J. 156 (1976) 71.
[3] A.L. Goldberg, J. Biol. Chem. 244 (1969) 3223.
[4] R.J. Zeman, R. Lundemann, J.D. Etlinger, Am. J. Physiol. 254 (1987) E152.
[5] F.W. Booth, P.D. Gollnick, Med. Sci. Sports Exerc. 15 (1983) 415.
[6] K. Furuno, M.N. Goodman, A.L. Goldberg, J. Biol. Chem. 265 (1990) 8550.
[7] G. Boissonneault, R.R. Tremblay, FEBS Lett. 257 (1989) 329.
[8] A. Jakubiec-Puka, J. Kordowska, C. Catani, U. Carraro, Eur. J. Biochem. 193 (1990) 623.
[9] D. Taillander, E. Aurousseau, D. Meynial-Denis, D. Bechet, M. Ferrara, P. Cottin, A. Ducastaing, X. Bigard, C.-Y. Guezennec, H.-P. Schmid, D. Attaix, Biochem. J. 316 (1996) 65.
[10] J. Appell, Sports Med. 10 (1990) 42.
[11] J.-C. Sanchez, D. Chiappe, V. Converset, C. Hoogland, P.-A. Binz, S. Paesano, R.D. Appel, S. Wang, M. Sennitt, A. Nolan, M.A. Cawthorne, D.F. Hochstrasser, Proteomics 1 (2001) 136.
[12] D. St-Pierre, P.F. Gardiner, Exp. Neurol. 90 (1985) 635.
[13] C.S. Giometti, N.G. Anderson, N.L. Anderson, Clin. Chem. 25 (1979) 1877.
[14] C.S. Giometti, M. Barany, M.J. Danon, N.G. Anderson, Clin. Chem. 26 (1980) 1152.
[15] C.S. Giometti, N.G. Anderson, Clin. Chem. 27 (1981) 1918.
[16] M. Wilm, A. Shevchenko, T. Houthaeve, S. Breit, L. Schweigerer, T. Fotsis, M. Mann, Nature 379 (1996) 466.
[17] U. Hellman, C. Wernstedt, J. Gonez, C.-H. Heldin, Anal. Biochem. 224 (1995) 451.
[18] R.J. Isfort, R.T. Hinkle, M.B. Jones, F. Wang, K.D. Greis, Y. Sun, T.W. Keough, N.L. Anderson, R.J. Sheldon, Electrophoresis 21 (2000) 2228.
[19] R.J. Isfort, F. Wang, K.D. Greis, Y. Sun, T.W. Keough, R.P. Farrar, S.C. Bodine, N.L. Anderson, Proteomics (2002) in press.
[20] H. Naito, S.K. Powers, H.A. Demirel, T. Sugiura, S.L. Dodd, J. Aoki, J. Appl. Physiol. 88 (2000) 359.